Electronic transport in alkali-tungsten bronzes

Itzhak Webman and Joshua Jortner
Department of Chemistry, Tel-Aviv University, Tel-Aviv, Israel

Morrel H. Cohen
James Franck Institute and Department of Physics, The University of Chicago, Chicago, Illinois 60637
(Received 21 April 1975)

In this paper we present a coherent physical picture of the electronic structure and the transport properties of alkali-tungsten bronzes, M_XWO_3, over the entire concentration range $X = 1$–0 of the alkali atoms. We propose a model based on nonrandom clustering of the alkali atoms into metallic regions characterized by the local atomic fraction $X_{\text{local}} = 1$. Provided that the M-M correlation length b considerably exceeds the lattice spacing, we can define a percolation problem in which a volume fraction $C = X$ of the material is occupied by the metallic regions, the remainder consisting of semiconducting regions. The threshold $C^* \simeq 0.17$ for continuous percolation marks the onset of the continuous metal-nonmetal transition in this microscopically inhomogeneous material. This physical picture is borne out by the available magnetic data. A semiquantitative calculation of the cluster stabilization energy with respect to the dispersed phase suggests that a negative surface energy exists between MWO_3 and WO_3 within a coherent WO_3 lattice. b is determined by the cluster size at which the metallic clusters begin to lose that stabilization energy. The Madelung energy provides a barrier against penetration of the electrons into the nonmetallic regions. Tunneling corrections are therefore negligible and we can define local electronic structure and transport properties. An analysis of the electrical conductivity data was carried out by utilizing the results of numerical simulations of the conductivity in simple-cubic lattices which incorporated correlation between metallic bonds. The numerical results were modified to account for scattering from the boundaries of the metallic regions. For low values of the conductivity ratio ($\sim 10^{-4}$) between the nonmetallic and the metallic regions, the effective-medium theory, modified to account for boundary scattering effects, faithfully reproduces the results of the numerical simulation for $C > 0.4$. An excellent fit of the available experimental conductivity data in the range $C = 0.9$–0.22 and over the temperature range 4–770°K has been obtained. In the process we found that the M-M correlation length is temperature independent and has the value of $b \simeq 45$ Å. The Hall effect and the Hall mobility were successfully analyzed utilizing a modified effective-medium theory.

I. INTRODUCTION

The physical properties of tungsten bronzes M_XWO_3 have been studied since 1823.[1] These materials are nonstoichiometric compounds with metal atoms of atomic concentration X partially occupying the simple cubic interstitial sites which, together with the WO_3 sites, make up a perovskite lattice.[2–5] In particular, the alkali-tungsten bronzes have been studied extensively over the last 25 years.[6,7] The electrical conductivity[7–10] and Hall effect[9–11] of Li_XWO_3, Na_XWO_3, and K_XWO_3, $0.2 < X < 1$, exhibit variations with X characteristic of a metal-nonmetal transition at $X \leq 0.2$. The conductivity, Fig. 1, shows practically no dependence on species of alkali atom or structural modification of the lattice. Above $X = 0.4$–0.5, σ increases linearly with T, $T > 20$ °K, and $d\sigma/dT$ depends weakly on X.[8] For $X < 0.1$, an activated temperature dependence of σ was observed.[7] The Hall coefficient R increases gradually with decreasing X down to $X \simeq 0.4$, increasing more rapidly for $0.3 \geq X \geq 0.2$, Fig. 1. Gardner and Danielson[11] fitted their Hall-effect data for $0.5 < X < 1$ to the approximate relation $R \propto X^{-1}$ following from the free-electron model. However, Lightsey's more recent data[10] for $0.22 < X < 0.4$ increase more steeply than predicted by the free-electron model. Semiquantitative studies[12] of the optical properties of Na_XWO_3 show striking changes between $X = 0.15$ and $X = 0.20$.

The variations of both the spin susceptibility and the specific heat[13–15] with X are incompatible with the free-electron model.[16] The values of the volume spin susceptibility calculated from the available experimental data,[7,13,14] Fig. 2, indicate a linear dependence of the density of states at the Fermi energy E_F on X and not the $X^{1/3}$ dependence expected from the free-electron model.

The low ^{23}Na Knight shift[17,18] observed for $X < 1$ indicates that the electrons have become dissociated from the alkali atoms. Detailed studies of transient NMR from ^{23}Na and ^{183}W by Fromhold and Narath[18,19] indicate that the electrons are transferred into states derived primarily from W $5d$ orbitals as proposed originally by Sienko.[7] It was, however, pointed out by Mackintosh[20] that the NMR properties of ^{23}Na in Na_XWO_3 are very similar to those of Be in beryllium metal,[21] where the long relaxation time T_1 and the small negative Knight shift originate predominantly from a p-type band. Thus the NMR data[17–19] for sodium-tungsten

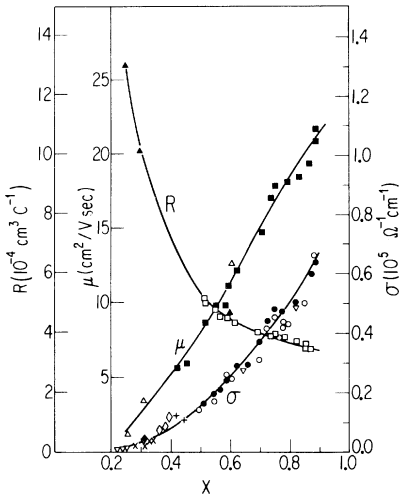

FIG. 1. Electronic transport data for alkali-tungsten bronzes at 300 °K. σ data: ×, ◇, cubic Li_XWO_3 (Ref. 6); ○, cubic Na_XWO_3 (Ref. 8); ●, cubic Na_XWO_3 (Ref. 9); ▽, cubic Na_XWO_3 (Ref. 10); +, tetragonal Na_XWO_3 (Ref. 6); ◆, tetragonal K_XWO_3 (Ref. 6). R data for cubic Na_XWO_3: □, (Ref. 9); ▲, (Ref. 10). μ data for cubic Na_XWO_3: ■, (Ref. 9); △, (Ref. 10).

bronzes do not provide unambiguous evidence for complete electron transfer to the W 5d band.[20] Theoretical evidence pertaining to the nature of the electronic structure of these materials comes from the band-structure calculations of Matheiss[22] on $K_{0.92}MoO_3$, which is presumably very similar to Na_XWO_3. These augmented-plane-wave (APW) calculations show that the Mo d bands are located below the K s and p bands.[23] Furthermore, the electronic structure proposed for $KMoO_3$, where the electrons are transferred into states originating from Mo 5d orbitals, accounts well[22] for the experimental data for the de Haas–van Alphen effect[24] in $Na_{0.93}MoO_3$ and $K_{0.92}MoO_3$, supporting the Sienko model[7] for the electronic structure of the alkali-tungsten bronzes.

The transient NMR data of Fromhold and Narath[18,19] indicate that there is substantial clustering of the Na atoms and not a uniform random distribution of Na atoms over simple-cubic interstitial sites. Indeed, their results[18,19] suggest a model in which substantially all of the Na atoms are clustered into sizable regions of local atomic fraction $X = 1$. The lack of dependence of Knight shift and relaxation time on X for the ^{23}Na nuclear resonance and the linear dependence of the specific heat and spin susceptibility on X all indicate such a model. The observed inhomogeneity of the environments of the Na nuclei reflects the presence of surface and interior atoms in the clusters. Similarly, there are interior, surface, and exterior W nuclei, consistent with the observed environmental inhomogeneity of the ^{183}W nuclei.

We are thus led by compelling experimental evidence via the penetrating analysis of Fromhold and Narath[18,19] to a picture of the alkali-tungsten bronzes closely similar to the picture of the metal-ammonia solutions (MAS) we have recently developed.[25] Both consist of metallic regions of correlation radius b randomly mixed with nonmetallic regions. We have systematically investigated the transport and other properties of such microscopically inhomogeneous materials[25,26] which undergo continuous metal-nonmetal transitions. We have developed quantitative theories of their electronic properties and applied them successfully to the interpretation and ordering of relevant data in expanded liquid Hg, liquid Te, MAS, and some liquid-alloy systems.[25,26]

This model of a random distribution of metallic regions having a correlation radius b within which X remains unity leads to an interpretation of the metal-nonmetal transition in terms of a threshold for continuous percolation and rules out the possibility of a Mott transition,[27] as the conduction electrons are always in regions which are locally

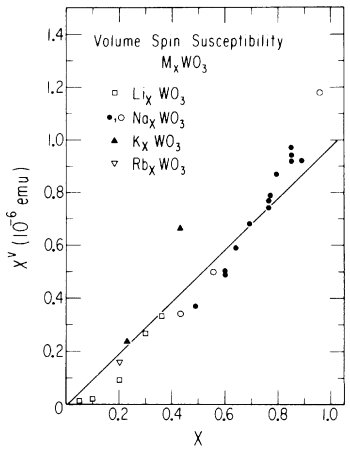

FIG. 2. Concentration dependence of the paramagnetic susceptibility of alkali-tungsten bronzes. The experimental molar susceptibility χ_m of M_XWO_3 was analyzed by setting $\chi_m = \chi_e + \chi(WO_3) + X\chi(M^+)$, where $\chi(WO_3) = -21\times10^{-6}$ emu/mole is the molar susceptibility of pure WO_3 (Ref. 13), $\chi(Li^+) = -0.7\times10^{-6}$ emu/mole, $\chi(Na^+) = -6.1\times10^{-6}$ emu/mole, $\chi(K^+) = -14.6\times10^{-6}$ emu/mole, and $\chi(Rb^+) = -22.0\times10^{-6}$ emu/mole are the molar susceptibilities of the alkali cations [C. Kittel, *Introduction to Solid State Physics* (Wiley, New York, 1953)]. χ_e is the molar susceptibility of the conduction electrons. The volume spin susceptibility is $\chi'' = \chi_e/V$, where the molar volume is $V = La^3/X$ and L is Avogadro's number. The lattice constant [B. W. Brown and E. Banks, J. Am. Chem. Soc. 76, 963 (1954)] is $a = 3.785 + 0.082X$ Å. Experimental data: □, Li_XWO_3 (Ref. 13b); ●, Na_XWO_3 (Ref. 14); ○, Na_XWO_3 (Refs. 7 and 13a); ▲, K_XWO_3 (Ref. 7); ▽, Rb_XWO_3 (Ref. 7).

metallic.

The notion of a percolation threshold in this system was first introduced by Mackintosh.[28] He proposed that the electrons moved through $3p$ states on randomly distributed Na atoms and that metallic conduction occurred above the percolation threshold for the site-percolation problem so defined on the simple cubic lattice of Na sites. This site-percolation model has been further developed by Fuchs,[16] who supposed the electron to be restricted to the vicinity of the Na atoms without specifying the detailed nature of the wave functions. He considered the Na atoms to be randomly distributed over the interstitial sites and developed approximate expressions for the conductivity based on percolation theory and interaction of the conduction electrons with "Na vacancies." He also supposed the Fermi level to be fixed by the requirement of close correlation of electrons with Na atoms leading to a density of states proportional to X, in agreement with magnetic and heat-capacity data. There are serious difficulties with the microscopic aspects of Fuchs' picture, but it contained much of the essential physics later developed by Kirkpatrick[29-31] and by Cohen and Jortner.[25,26] With regard to the difficulties, the nuclear-spin dynamics require nonrandom clustering. The electrons do not move on the Na atoms.[7,23b] The transport analysis is internally inconsistent; electrons cannot both be localized on Na atoms and scatter off vacancies in a free-electron-like way; and the low-temperature and high-temperature transport were treated differently. The conductivity is not simply proportional to the percolation probability as shown by Thouless and Last[32] and by Kirkpatrick.[29-31] Finally, the site-percolation threshold is too high, corresponding to a value of $X = X^*$ of 0.33 for a simple cubic lattice.[33]

Kirkpatrick[30] pointed out that his analysis of transport in disordered systems as a percolation process applied also to the alkali-tungsten bronzes. Recently, Lightsey[10] demonstrated that his detailed conductivity data were consistent with Kirkpatrick's power law[29-31]

$$\sigma \propto (X - X^*)^{1.6} , \tag{1.1}$$

with a percolation threshold $X^* = 0.17$. Once again, he supposed the Na were randomly distributed and that the electrons moved from Na to Na, defining a site-percolation problem. He proposed electron transfer to nearest and next-nearest neighbors, giving an effective number of nearest neighbors of 14 to account for the low value of X^*.

In the present paper, we apply our previous methods of analysis to the Na cluster model of the alkali-tungsten bronzes. We carry out here a detailed analysis of a continuous metal-nonmetal transition in a solid over a broad temperature range. We find excellent agreement with theory for the electrical conductivity and Hall coefficient. In the process, we find that the Na-Na correlation distance is practically temperature independent and has a value of roughly 45 Å.

II. CLUSTER MODEL FOR ALKALI-TUNGSTEN BRONZES

For each simple cubic interstitial site l we can define a site occupation number n_l which takes the values $n_l = 1$ or $n_l = 0$ according to whether an alkali atom is or is not at that site. The mean site occupation number is

$$\bar{n} \equiv \langle n_l \rangle = X . \tag{2.1}$$

We define further a conditionally averaged site occupation number

$$A(|\vec{r}_m - \vec{r}_l|) = \langle n_m | n_l = 1 \rangle - X , \tag{2.2}$$

which is the difference between the mean value of the occupation number on site m subject to the condition that site l is occupied by an alkali atom and the mean occupation number X. In the cluster model, $A(R)$ is $1 - X$ for $R = 0$, remains near that value for $R \simeq b$, and drops rapidly to zero for $R \geq b$. This behavior is sketched in Fig. 3. Provided b is substantially larger than the lattice constant a, we can treat $A(R)$ as a continuous function, as in Fig. 3. We can idealize the cluster model further by replacing $A(R)$ by the simple step function

$$\begin{aligned} A(R) &= 1 - X , \quad R \leq b , \\ A(R) &= 0 , \quad R > b . \end{aligned} \tag{2.3}$$

In this model there is a local value of X, $X_l = n_l = 1$, within the clusters which drops abruptly to zero at the cluster boundary.

Roughly speaking, space is divided into statistically independent regions of diameter $2b$, within

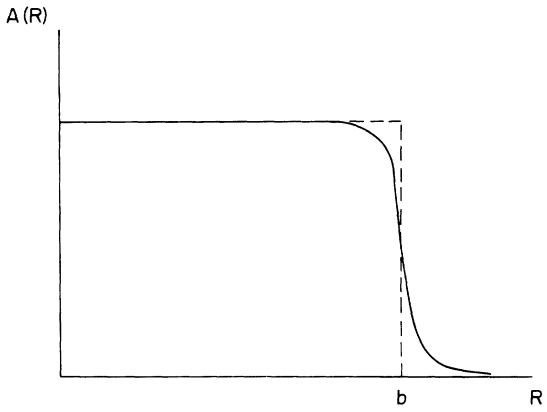

FIG. 3. A schematic representation of the conditionally average site occupation number $A(R)$ for the nonrandom cluster model.

which the local occupation number fluctuates randomly between 0 and 1,

$$n_l = 1 \text{ with probability } X ,$$

$$n_l = 0 \text{ with probability } (1 - X) .$$

Because we are supposing b substantially larger than a, n_l may be regarded as a continuous variable n. This defines a continuous percolation problem for which the percolation threshold is[34,35] $X^* = 0.15-0.17$. There are local metallic regions ($n = 1$) occupying a volume fraction $C = X$ of the material and insulating regions ($n = 0$) occupying a volume fraction $1 - C$. Above the percolation threshold there are continuous metallic paths extending throughout the material. Below the percolation threshold, only isolated metallic clusters exist. The percolation threshold marks the onset of a continuous metal-nonmetal transition within the microscopically inhomogeneous material.

We have now made contact with the previous analysis of Cohen and Jortner (CJ) of such transitions.[25,26] The density of states $n(E_F)$ at the Fermi energy is given by

$$n(E_F) = Cn_0(E_F) , \tag{2.4}$$

where $n_0(E_F)$ is the density of states for pure $NaWO_3$. Fuchs[16] was the first to propose this relation, justifying it on the basis of the Fermi-Thomas model; CJ have given a more precise derivation and interpretation. It is valid when the shorter of the phase-coherence length or the Fermi wavelength is small compared to b, when it becomes an expression of the Weyl theorem.[36] Equation (2.4) gives an immediate explanation of the spin susceptibility and the specific-heat data with $C = X$.

A major difference between the present solid material and the previous liquid systems studied by CJ is the absence of motional narrowing of the Knight shift. In the liquid case the Knight shift was given by an equation of the form (2.4), and provided a convenient basis for the determination of C. In the present case the ^{23}Na nuclei are in a time-independent environment in which the Knight shift κ, a local property, has the full metallic value κ_0, independent of C.

Having given the cluster model a precise formulation which makes contact with the previous CJ theory, before going on to apply that theory to the alkali-tungsten bronzes, we first examine the physical origin of the clustering. We consider those terms in the total energy of the system which depend on the configuration of the alkali atoms. We evaluate these per alkali atom in a rough way to obtain an indication of whether a uniform or a clustered configuration is stabler at $T = 0\,^\circ K$.

The energy contains two parts, a single-particle band-structure energy arising from the transfer of electrons from the Na atoms to the tungsten atoms, and a Coulomb interaction energy. The band model we use for evaluating the former consists of a threefold degenerate (choosing $5d - t_{2g}$ bands following Sienko[7]) semicircular density of states (per W atom)

$$n(E) = \frac{24}{\pi B}\left[1 - \left(\frac{2E}{B}\right)^2\right]^{1/2} , \tag{2.5}$$

where B the bandwidth and E measured relative to the center of the band. Later, in making energy comparisons, we take the bottom of the band as the origin of single-particle energy. The Fermi energy is determined from

$$\int_{-B/2}^{E_F^U} n(E)\, dE = X . \tag{2.6}$$

We wish to discover whether the clustered configuration is stabler than the dispersed configuration for all X. To do so, it is sufficient to prove it for small X, for which (2.6) yields

$$X = 4(\theta_F^U)^3/\pi , \tag{2.7}$$

where

$$\cos\theta_F^U = 2\left|E_F^U\right|/B . \tag{2.8}$$

The single-particle band-structure energy is

$$E_1^U = \int_{-B/2}^{E_F^U} En(E)\, dE . \tag{2.9}$$

Inserting (2.7) and (2.8) into (2.9) gives

$$E_1^U = \tfrac{1}{2} BX , \tag{2.10}$$

which can be neglected for low X. In the dispersed configuration, each Na ion is screened, either by a localized state or by a Fermi-Thomas screening cloud, depending on the value of X. We estimate the latter energy by supposing that the screening cloud is restricted to the eight nearest-neighbor W atoms, the most favorable case. The Coulomb interactions of the $\frac{1}{8}$ of an electron charge on each atom with the Na ion is reduced by about a factor of 2 by their mutual repulsion and the energy of polarization. The screening energy E_2^U becomes

$$E_2^U = -(1/\sqrt{3})\, e^2/a . \tag{2.11}$$

Within a large cluster, the energy per Na atom consists of E_1 evaluated for $X = 1$,

$$E_1^c = (2/\pi)B \sin^3\theta_F^c , \tag{2.9'}$$

$$1 = (3/\pi)(2\theta_F^c - \sin 2\theta_F^c) . \tag{2.6'}$$

Solving (2.6′) yields

$$\theta_F^c = 0.313 , \tag{2.12}$$

$$E_1^c = 0.366B . \tag{2.13}$$

The Coulomb interaction energy is just a Madelung

energy for the Na^+ ions and the conduction electrons which are restricted to the W atoms. Together these form a CsCl structure so that the latter energy is

$$E_2^c = -1.76\, e^2/a \,. \tag{2.14}$$

Equation (2.6) yields the expression

$$B = 24 \sin\theta_F^c/\pi n(E_F) \,. \tag{2.15}$$

We need here the band density of states, whereas the specific heat contains the electron-phonon renormalization factor $(1+\lambda)$. Because, however, the density of states estimated from the specific heat agrees with that from the spin susceptibility to 20% or better, we can ignore λ. The specific heat yields[15,19] accordingly a value of $n(E_F)$ of 8.2×10^{11} (cgs) for $X=1$. Inserting that value of $n(E_F)$ and (11 – 13) into (11 – 15) yields 4.8 eV for B. The value of a is 3.85 Å. Adding (2.13) and (2.14) and comparing the result with (2.11) leads us to the conclusion that $X=1$ clusters are stable with respect to a dispersed phase by 2.7 eV per Na atom.

This stabilization energy at $T=0$ is so large that it raises the possibility of macroscopic precipitation of a $M\mathrm{WO_3}$ phase. Although these materials are prepared at elevated temperatures (700–800 °K), it can be easily demonstrated that the configurational entropy is unimportant. The maximum value of the entropy of mixing in the cluster configuration is $-TS = -kT \ln 2$, 0.04 eV at 700 °K, which is considerably lower than the cluster stabilization energy at $T=0$. Thus the configurational entropy cannot destabilize macroscopic precipitates with respect to microscopic clusters. On the basis of experimental information we can reject the possibility that microscopic clusters are metastable and that diffusion effectively ceases above the temperature of precipitation. The diffusion coefficient[5] (for vacancies) in $\mathrm{Na}_X\mathrm{WO_3}$ is 2×10^{-15} $\mathrm{cm^2 sec^{-1}}$ at 770 °K, so that the diffusion length on a time scale of 24 h is 1 μm. This would imply that the precise value of the correlation length b depends on the thermal history of the sample, and, as we shall see, the transport properties of the material are sensitive to the value of b. On the other hand, the electrical conductivity data for $M_X\mathrm{WO_3}$ are insensitive to thermal annealing for 24 h at 700 °K.[8] We are inevitably led to the conclusion that the cluster configuration is stable both with respect to dispersion into a uniform phase of the average composition and with respect to growth of clusters into precipitates. Such stability against precipitation would be ensured by a negative surface energy associated with the interface between $M\mathrm{WO_3}$ and $\mathrm{WO_3}$ within a coherent $\mathrm{WO_3}$ lattice. A negative surface energy drives the clusters towards smaller radii. The correlation length b would presumably be determined by the size at which a cluster begins to lose the Madelung stabilization energy and/or its band energy increases. Such a picture is akin to a phase separation on a microscopic scale, where the dispersed phase, consisting of $M\mathrm{WO_3}$ clusters, is characterized by a negative surface energy.

It would be of interest to improve our rough estimate of the stabilization energy by basing it on an accurate band structure and a detailed screening calculation. More important, the conjecture of negative surface energy has to be quantitatively examined by considering the band energy and the Madelung energy near the cluster interface. Supposing that such detailed studies confirm our rough argument, it should be noted that the latter is quite general. Clustering can be expected whenever an electron is transferred from a metal atom into states which do not overlap the metal atom appreciably. If, on the other hand, such overlap were to occur, the metal atom would be locally neutral and insensitive to its configuration. Dispersion would then be favorable.

We now consider the applicability of the CJ formulation of transport theory for inhomogeneous systems to the present case. An essential requirement is that the conduction electrons are indeed confined to what we have called the "metallic" regions. The Madelung energy provides a potential barrier against penetration of the electrons into the "nonmetallic" regions of 6.6 eV in the present case. The Fermi energy is about 1.3 eV (cf. Sec. III), and the tunneling barrier for electrons at the Fermi level is therefore 5.3 eV. With such a barrier, tunneling can be expected to be completely negligible as long as b is greater than a.

III. ELECTRICAL TRANSPORT IN ALKALI-TUNGSTEN BRONZES

The cluster model for $M_X\mathrm{WO_3}$ bronzes outlined above implies that electronic transport in these materials is amenable to an approximate description with the aid of semiclassical percolation theory. Within the semiclassical approximations, the transport problem becomes equivalent to conduction in a macroscopically inhomogeneous medium. Kirkpatrick[29,30] carried out a numerical study of the conductivity σ of a simple cubic network of resistors in which each nearest-neighbor bond was randomly assigned a conductance σ_0 with probability C and σ_1 with probability $1-C$. The conductivity ratio is $x = \sigma_1/\sigma_0$. In the limit $x=0$, the current flow within the resistor network reduces to a bond percolation problem, for which the percolation threshold is $C^* = 0.25$[33] and where numerical calculations result in

$$\sigma(C) = 0 \,, \quad 0 < C < 0.25 \,, \tag{3.1a}$$

$$\sigma(C) = A(C - 0.25)^{1.6} \,, \quad 0.25 < C < 0.4 \,, \tag{3.1b}$$

$$\sigma(C) = \sigma_0(\tfrac{3}{2}C - \tfrac{1}{2}) \ , \quad 0.4 < C < 1.0 \ . \tag{3.1c}$$

In simulating electrical transport properties of a microscopically inhomogeneous material we are dealing with a continuous site-percolation problem in which any portion of the material can be randomly metallic or nonmetallic. To mimic the features of the continuous percolation problem one can impose correlations on neighboring bonds, so that if a bond is of one type all its neighbors out to the correlation distance b must be of the same type. We have carried out a numerical study of the conductivity of simple cubic resistor network with correlated bonds.[35] We now briefly outline the results for the conductivity of a randomly inhomogeneous conductor containing regions of two finite but widely different values of the local conductivity. Typical numerical results obtained for correlated network model incorporating nearest-neighbor and second-nearest-neighbor bond correlation are portrayed in Fig. 4. These data are compared with Kirkpatrick's results for the uncorrelated network and with the prediction of effective-medium theory.[37,26] The major effects of correlation is to shift the percolation threshold from 0.25 to $C^* = 0.15 \pm 0.02$, in accord with numerical simulations of the percolation probability[34,35] for the continuous percolation problem. The macroscopic conductivity σ was expressed in the form

$$\sigma = \sigma_0 f(x, C) \ , \qquad x = \sigma_1/\sigma_0 \ , \tag{3.2}$$

where σ_0 and σ_1 correspond to the conductivities at $C = 1$ and at $C = 0$, respectively. The effective-medium theory (EMT) for the conductivity[25,26,29,37]

$$f(x, C) = a + (a^2 + \tfrac{1}{2}x)^{1/2} \ , \qquad a = \tfrac{1}{2}[(\tfrac{3}{2}C - \tfrac{1}{2})(1 - x) + \tfrac{1}{2}x] \ , \tag{3.3}$$

was found accurate for $0.4 < C < 1.0$ for all values of the conductivity ratio x, in agreement with Kirkpatrick's original work.[29] Serious deviations from the EMT occur for $C < 0.4$ for small values of x (< 0.03). This is not surprising, as the EMT, which rests on a mean-field approximation for the local conductivity, overestimates the percolation threshold for $x = 0$, $C^*_{\mathrm{EMT}} = \frac{1}{3}$, and can in general be expected to result in too low values of σ for $C < 0.4$ and $0 \leq x < 3 \times 10^{-2}$.

In the range $0 < C < 0.4$, two classes of materials are encountered: (a) For materials characterized by a high conductivity ratio $x > 3 \times 10^{-2}$ the EMT, Eq. (3.3), faithfully reproduces the numerical results throughout the whole C range. (b) For materials characterized by a low conductivity ratio, $x \leq 5 \times 10^{-4}$, Kirkpatrick's scaling law

$$f(x, C) = A(C - C^*)^{1.6} \ , \quad C^* < C < 0.5 \ , \quad A \simeq 1.6 \ , \tag{3.4}$$

is obeyed above the percolation threshold. For low values of $C (< 0.1)$ the conductivity is given by

$$f(x, C) = x/(1 - C/C^*) \ . \tag{3.5}$$

In view of the 10% uncertainty in the value of C^* for the continuous percolation problem,[34,35] the best procedure to analyze the conductivity data for a microscopically inhomogeneous material which corresponds to class B is to adopt the EMT for $C > 0.4$ and utilize the results of numerical simulations for $C < 0.4$.

These quantitative classical results for the conductivity are applicable provided that the phase-coherence length of the conduction electrons within the metallic regions is considerably shorter than the correlation length b. For Na_xWO_3 bronzes near $X = 1$, the conductivity is $\sim 10^5$ $(\Omega\,\mathrm{cm})^{-1}$ and the metallic regions correspond to the propagation regime where the mean free path l considerably exceeds the lattice spacing. In that case scattering of metallic cluster boundaries[25] reduces the local conductivity $\sigma_0(C)$ below the metallic conductivity σ_0 of the homogeneous material at $C = 1$. A modified theory, which incorporates boundary scattering results in the change of Eq. (2.2) to[25b]

$$\sigma = \sigma_0 D(C) \bar{f} \ , \tag{3.6a}$$

$$\bar{f} = f(C, x(C)) \ , \tag{3.6b}$$

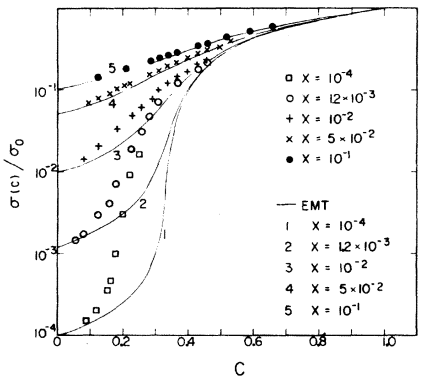

FIG. 4. Results for numerical simulations of continuous percolation. The conductivity of a simple cubic network of conductances σ_0 and σ_1 with nearest neighbor band correlation was calculated for a $18 \times 18 \times 18$ network. Values of the conductances are $\sigma_0 = 1$ (with probability C) and $\sigma_1 = 10^{-1}$, 5×10^{-2}, 10^{-2}, 1.2×10^{-3}, and 10^{-5} (with probability $1 - C$). The percolation threshold for this model is $C^* = 0.18$, reducing to $C^* = 0.15 \pm 0.02$ when spatial propagation of bond correlation to second-nearest neighbors is incorporated. The results of the numerical simulations are compared with the EMT, Eq. (3.3).

$$D(C) = z/[(1-C)+z] , \tag{3.6c}$$

$$x(C) = x/D(C) , \tag{3.6d}$$

$$z = 2b/l . \tag{3.6e}$$

Equations (3.6) and (3.3) constitute a modified effective-medium theory (EMT-z). For materials of class A, the EMT-z is applicable throughout the entire range $0<C<1$. For materials of class B, the EMT-z is valid only for $0.5<C<1.0$, while for $C<0.5$ we have utilized Eq. (3.6) where $\bar{f}$, Eq. (3.6b), was obtained from numerical simulations of σ/σ_0 in a correlated cubic network, with $x(C)$ given by Eq. (3.6d).

We are now in a position to analyze the conductivity data for alkali-tungsten bronzes. Fitting the theory to the experimental transport properties of the microscopically inhomogeneous material requires the following information: (a) Identification of the limits of the inhomogeneous transport regime, (b) establishing the relation between C and the composition X, and (c) determining the values of the transport coefficients at the limits $C=0$ and $C=1$. We have already considered (a) and (b) in Sec. II, where we have shown that M_XWO_3 bronzes are microscopically inhomogeneous throughout the entire composition range $0<X<1$ and that $C=X$. What is now required is an estimate of the conductivity ratio $x=\sigma_1/\sigma_0$, where σ_1 and σ_0 are the local conductivities in the metallic and the semiconducting regions, respectively. A rough estimate of the local conductivity σ_1 in the semiconducting regions can be obtained from the experimental data[38] for pure WO_3. The electrical properties of WO_3 were explained as that of an extrinsic semiconductor with shallow donor levels originating from interstitial metal atoms. The highest value of the conductivity recorded for different samples at 300 °K is ~5 $(\Omega\,\mathrm{cm})^{-1}$, which may be taken as an order of magnitude estimate for σ_1. A linear extrapolation of the conductivity data to $C=X=1$ results in the preliminary estimate $\sigma_0 \sim 7\times10^4\,(\Omega\,\mathrm{cm})^{-1}$ at 300 °K, so that $x\sim10^{-4}$. This low value of the conductivity ratio implies that alkali-tungsten bronzes correspond to materials of class (b).

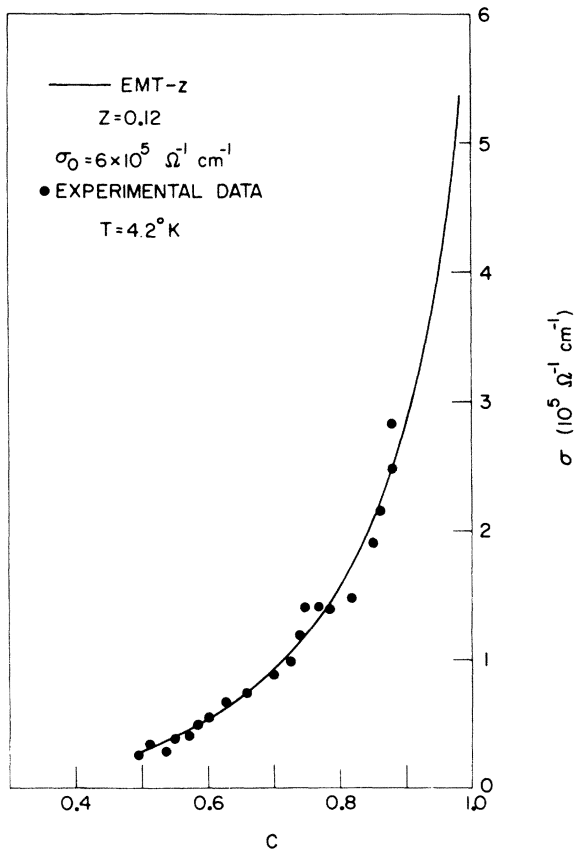

FIG. 5. Analysis of the electrical conductivity data of Na_XWO_3, $0.5<X<1.0$ at 4.2 °K (Refs. 8 and 9) in terms of the modified effective-medium theory (EMT-Z), Eq. (3.5) and (3.6). The best fit obtained for $\sigma_0=6\times10^5$ $(\Omega\,\mathrm{cm})^{-1}$ and $z=0.12$ is shown by the solid curve.

Our numerical simulations show that the EMT holds accurately for $0.4<C<1.0$. Moreover, the EMT in this composition range reduces to its $x=0$ form

$$\sigma/\sigma_0 = (\tfrac{3}{2}C - \tfrac{1}{2}) , \quad x<5\times10^{-3} , \quad 0.4<C<1 \tag{3.7}$$

for low values of x as we are dealing with here. Accordingly, we have attempted to correlate the experimental data at 4.2, 300, 523, and 773 °K for $0.5<C<1$, summarized in Figs. 5–7 with Eq. (3.7), which just implies a linear σ-vs-C relation at each temperature. The experimental σ data at 4.2 and at 300 °K fall systematically below the linear σ-vs-C relation at constant T implied by the EMT. We have therefore fitted the data to the EMT-z, Eqs. (3.6a)–(3.6b), which for the present case takes the form

$$\sigma = \sigma_0(\tfrac{3}{2}C - \tfrac{1}{2})z/[(1-C)+z] , \quad x<5\times10^{-3} , \quad 0.5<C<1.0 . \tag{3.8}$$

We have adjusted two parameters σ_0 and z at each temperature to get the best fit. A least-square analysis results in the values of σ_0 and z summarized in Table I. The results are shown in Figs. 5–7. The fit to the EMT-z is excellent at 4.2 and at 300 °K. At higher temperatures, z is sufficiently large so that there is little difference between the EMT, Eq. (3.7), and the EMT-z, Eq. (3.8).

The conductivity σ_0 at $C=1$ is

$$\sigma_0 = e^2Sl/4\pi^3\hbar , \tag{3.9}$$

where S is the area of the Fermi surface. Equations (3.6e) and (3.9) result in

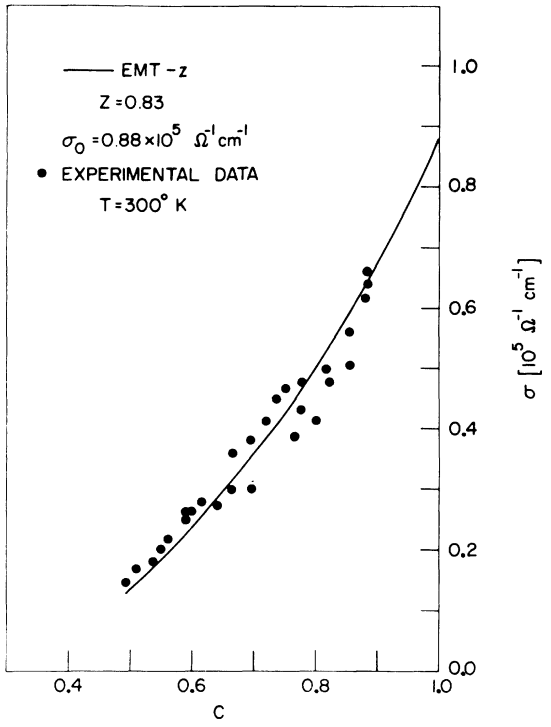

FIG. 6. Analysis of the electrical conductivity data of Na_XWO_3, $0.5 \leq X < 1.0$ at 300 °K (Refs. 8–10) in terms of the modified effective-medium theory (EMT-Z), Eqs. (3.5) and (3.6). The best fit obtained for $\sigma_0 = 0.88\ (\Omega\,\text{cm})^{-1}$ and $z = 0.83$ is shown by the solid curve.

$$\sigma_0 z = e^2 S b / 2\pi^3 \hbar\ . \tag{3.10}$$

The quantity $\sigma_0 z$ is independent of temperature over a broad range, as is evident from the data summarized in Table I. For our model of alkali-tungsten bronzes, the metallic volume fraction C remains equal to X, independent of temperature. The local electronic structure remains that of MWO_3 so that S in (3.9) and (3.10) is temperature independent. The constancy of $\sigma_0 z$ implies that b is temperature independent, an important result which is consistent with our proposal of negative surface energy.

From these values of z a rough estimate can be obtained for b. From Eq. (3.10), we have $b = (2\pi^3\hbar/e^2 S)(\sigma_0 z)$, where $\sigma_0 z = 7.2 \times 10^4\ (\Omega\,\text{cm})^{-1}$, as obtained from Table I. For S, we take $4\pi k_F^2$, where k_F is the radius of a sphere in k space holding $\frac{1}{3}$ of an electron per W atom in each of the three bands. The corresponding value of b is

$$b = 45\ \text{Å}\ . \tag{3.11}$$

This result is of considerable interest, as rough quantitative microscopic structural information has been obtained from electrical conductivity data in the composition range where the EMT-z is applicable.

TABLE I. Parameters from analysis of electrical-conductivity data for alkali-tungsten bronzes.

T (°K)	σ_0 $[(\Omega\,\text{cm})^{-1}]$	z from $\sigma(C)$	$\frac{1}{\sigma_0}\frac{d\sigma_0}{dT}$ (°K^{-1})	z from $\frac{d\ln\sigma}{dT}$	$z\sigma_0$ [a]
4.2	6.0×10^5	0.12			0.72×10^5
300	0.88×10^5	0.83	4.8×10^{-3}	0.4	0.73×10^5
523	0.42×10^5	1.8	2.4×10^{-3}	1.5	0.75×10^5
773	0.26×10^5	2.8	1.7×10^{-3}	3.1	0.73×10^5

[a] z is taken from the concentration dependence of σ.

We are now able to provide an adequate interpretation of the available experimental data for the temperature dependence of the conductivity[8] in the range 300–800 °K for $0.88 > C > 0.49$. The temperature coefficient of σ is

$$\gamma(C, T) = \frac{1}{\sigma(C, T)} \frac{\partial \sigma(C, T)}{dT}\ , \tag{3.12}$$

and from Eqs. (3.8) and (3.10) we have

$$\gamma(C, T) = \frac{1}{\sigma_0(T)} \frac{d\sigma_0(T)}{dT} \left(\frac{z(T)}{1 - C + z(T)} \right)\ . \tag{3.13}$$

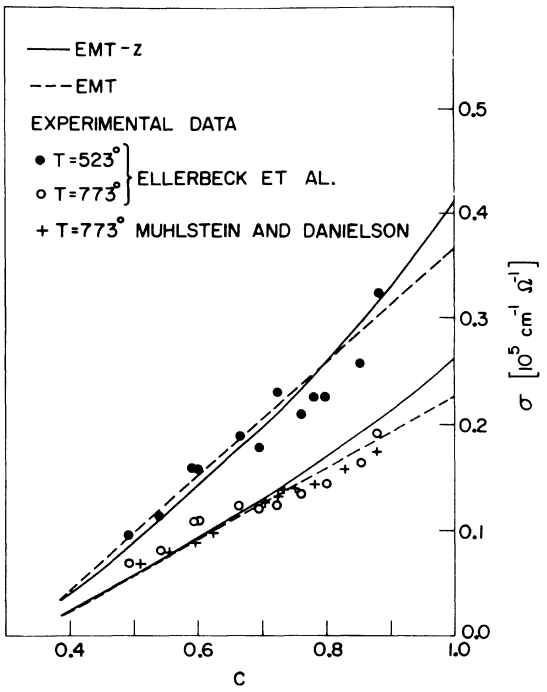

FIG. 7. Analysis of the electrical conductivity of Na_XWO_3, $0.5 \leq X < 1.0$ at 523 K and 773 °K (Refs. 8 and 9) in terms of the EMT-z (solid curves) and the EMT (dashed curves). The EMT-Z was fit taking $\sigma_0 = 0.42 \times 10^5\ (\Omega\,\text{cm})^{-1}$ and $z = 1.8$ at 523 °K and $\sigma_0 = 0.26 \times 10^6\ (\Omega\,\text{cm})^{-1}$ and $z = 2.8$ at 770 °K. The EMT Eq. (3.5), utilizes the values of $\sigma_0 = 0.37\ (\Omega\,\text{cm})^{-1}$ at 523 °K and $\sigma_0 = 0.23\ (\Omega\,\text{cm})^{-1}$ at 773 °K.

Thus, the composition dependence of r originates from the temperature dependence of z. Above 300 °K, the temperature coefficient of σ was expressed in the form $r(C, T) = -(a_1 + 2a_2T)/(a_0 + a_1T + a_2T^2)$, where the coefficients a_0, a_1, and a_2 were tabulated by Ellerbeck *et al.*[8] and T is given in degrees centigrade. From the linear plots of $[r(C, T)]^{-1}$ vs $(1 - C)$ at constant T, Fig. 8, we have obtained the values of z presented in Table I. These data derived from the temperature coefficient of the conductivity are in reasonable agreement with the z values obtained from the composition dependence of the conductivity. We have thus obtained so far a coherent quantitative interpretation of the conductivity data throughout the range $0.5 < C < 0.9$.

The effective medium theory breaks down at C values lower than 0.5 and the EMT-z is little different there. We have analyzed in Fig. 9 all the available experimental conductivity data in the range $0.22 \leq C < 0.9$ at 300 °K utilizing the results of numerical simulations corrected for boundary scattering effects. In the range $C = 0.22$–0.5 we have used the numerical results for $\bar{f}(x(C), C)$ [Eq. (3.6b)], where $x(C) = x/D(C)$, as simulated for a cubic network with correlated bonds. We have chosen $x = 10^{-4}$, which corresponds to our rough estimate of x given above, but the numerical results for $C > 0.22$ are not sensitive to the precise value of x for $x \leq 5 \times 10^{-4}$. From the available experimental information, a more accurate value of the conductivity ratio cannot be determined. Above $C < 0.5$ $\bar{f}(x(C), C)$ is again taken from the EMT-z, which faithfully reproduces the numerical results. An excellent fit between the experimental data and the results of numerical simulations is obtained over more than two orders of magnitude variation in σ. The conductivity data exhibit the variation expected for the continuous percolation problem. We feel that these results provide overwhelming support for the validity of the cluster model for alkali-tungsten bronzes.

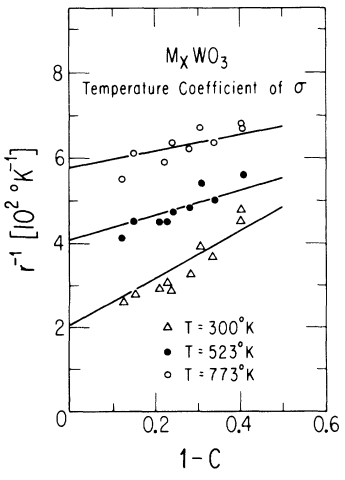

FIG. 8. Linear plots of the reciprocal value of the temperature coefficient of the conductivity, Eq. (3.11) vs $(1 - C)$ for $T = 300$, 523, and 773 °K. Data from Ref. 8.

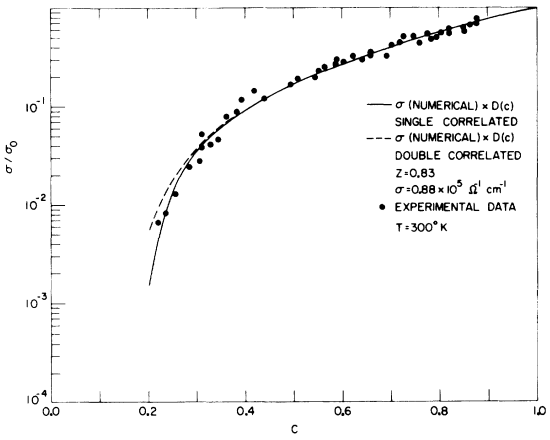

FIG. 9. Analysis of all the available electrical conductivity data of Na_XWO_3 at 300 °K in the range $0.22 < X < 0.9$. The experimental points were normalized by $\sigma_0 = 0.88 \times 10^5$, which corresponds to the values extracted from the analysis of σ via the EMT-Z in the high ($C > 0.5$) range. The solid curve represents the results of numerical simulations (with $x = 10^{-4}$) for the conductivity in a sc network incorporating nearest-neighbor bond correlations and introducing boundary scattering corrections with $z = 0.83$.

Hall-effect data are available for Na_XWO_3 in the composition range $X = 0.87$–0.22. The EMT yields[40] for the Hall coefficient R and for the Hall mobility μ

$$\begin{aligned} &\mu/\mu_0 = g(x, y, f) = [1 - B(1 - xy)]f^{-1}, \\ &R/R_0 = h(x, y, f) = [1 - B(1 - xy)]f^{-2}, \\ &B = \frac{(2f+1)^2(1-C)}{(2f+1)^2(1-C) + (2f+x)^2C}, \\ &y = \mu_1/\mu_0, \end{aligned} \tag{3.14}$$

where μ_0 and μ_1 are the Hall mobilities in the metallic and in the semiconducting regions, being given by the Hall mobilities at $C = 1$ and at $C = 0$, respectively. EMT-z yields correspondingly[25]

$$\begin{aligned} &R = \bar{h}R_0, \quad \mu = \bar{g}D(C)\mu_0, \\ &\bar{g} = g(C, x(C), y(C), \bar{f}), \quad \bar{h} = \bar{g}/\bar{f}, \\ &x(C) = x/D(C), \quad y(C) = y/D(C). \end{aligned} \tag{3.15}$$

In the interpretation of the electrical transport data of Na_XWO_3 we are interested in low values of x, $\simeq 10^{-4}$. On the basis of numerical simulations of σ we have concluded that the EMT or the EMT-z hold for $C > 0.4$ and we infer that the same will apply for R and μ. In the range $0.4 < C < 1.0$, μ and

R are close to their $x=0$ value, and these transport properties are practically independent of y. We also note that boundary scattering corrections do not affect the value of R in this range of C. For $C<0.4$ for low values of C, as we are concerned with here, the EMT or the EMT-z provide only a qualitative interpolation formula. A quantitative formal theory or numerical simulation is not yet available for the galvanomagnetic properties below $C=0.4$. We can, however, make an intelligent guess for the behavior of R and μ in the low range of C (<0.1). There EMT yields

$$\sigma/\sigma_0=(1-C/C^*_{\mathrm{EMT}})^{-1}\,, \tag{3.16}$$

$$R/R_0=(y/x)(1-C/C^*_{\mathrm{EMT}})^2+(3-C/C^*_{\mathrm{EMT}})^2(1-xy)C\,, \tag{3.17}$$

$$\mu/\mu_0=y(1-C/C^*_{\mathrm{EMT}})+x(3-C/C^*_{\mathrm{EMT}})^2 \times(1-C/C^*_{\mathrm{EMT}})^{-1}(1-xy)C\,, \tag{3.18}$$

where $C^*_{\mathrm{EMT}}=\frac{1}{3}$ is the percolation probability in the EMT. If we reinterpret Eq. (3.16) by replacing the EMT value of C^* by the actual value of 0.17, we obtain Eq. (3.5) for the conductivity at low C. In a similar way we shall replace C^*_{EMT} by $C^*=0.17$ in Eqs. (3.17) and (3.18) for R and μ. As we shall subsequently show that $y/x\sim10^4$ for alkali-tungsten bronzes we get

$$R=R_1(1-C/C^*)^2\,,\qquad \mu=\mu_1(1-C/C^*)\,, \tag{3.19}$$

for $0<C\leq0.1$ in this system. Unfortunately, no data are available for $C=X\leq0.1$.

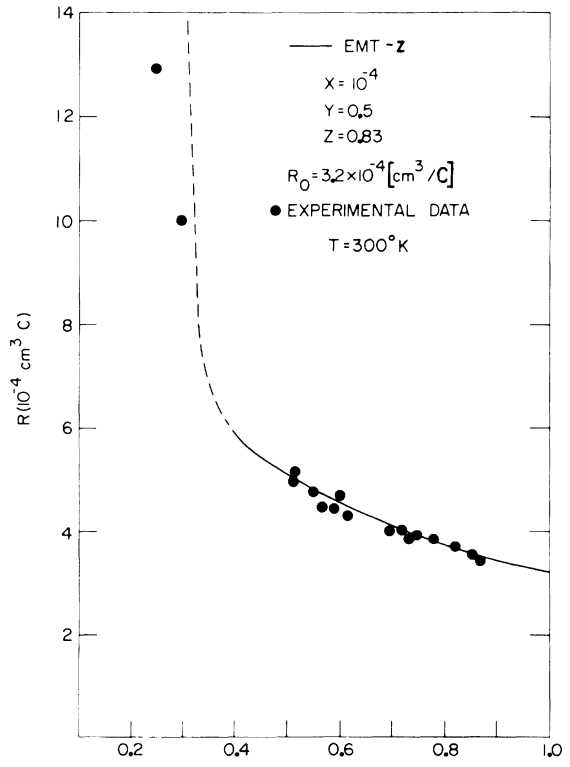

FIG. 10. Analysis of the Hall-effect data (Refs. 9 and 10) for Na_xWO_3 at 300 °K in terms of the effective-medium theory. Solid line presents the calculation by the EMT, Eq. (3.13), of the EMT-Z, Eqs. (3.14) and (3.15), with $x<10^{-3}$, and corresponds to the range $0.4<C<1$, where the effective-medium theory is reliable. Dashed line for $C<0.4$ represents the calculation of R via the EMT-Z, with $x=10^{-4}$, $y=0.5$, and $z=0.83$.

In the absence of a quantitative theory or numerical simulations for the galvanomagnetic properties we have compared the available data for Na_xWO_3 at 300 °K with EMT-z. A linear extrapolation of the Hall data to $C=X=1$ results in the estimate $R_0\simeq3\times10^{-4}$ cm^3 C^{-1} which together with the value $\sigma_0=0.88\times10^5$ $(\Omega\,\mathrm{cm})^{-1}$ at 300 °K results in $\mu_0\simeq28$ cm^2 V^{-1} sec^{-1}. The value of μ_1 can be roughly estimated from the Hall mobility[38] in pure WO_3, $\mu_1\sim16$ cm^2 V^{-1} sec^{-1}.

Thus $y=\mu_1/\mu_0\sim0.5$, as appropriate for a material undergoing a continuous metal-semiconductor transition, where we expect y to be of the order of unity. In Fig. 9 we present the available Hall-effect data together with the fit to the EMT-z for $0.22<C<1.0$. In the range $0.4<C<1$, this fit is identical to the EMT, resulting in the simple relation $R/R_0=4/(3C+1)$. A good fit of the Hall-effect data in the range $C>0.4$ was obtained by taking $R_0=3.1\times10^{-4}$ cm^3 C^{-1}, while the two experimental points available in the range $0.2<C<0.4$ can be qualitatively fit by the EMT-z with the values $x=10^{-4}$ and $z=0.83$ obtained from the analysis of conductivity data together with $y=0.5$. It should be borne in mind that in the latter range the EMT-z provides only qualitative guidance for the variation of R with C.

In view of the quantitative agreement of σ and R with the predictions of the EMT-z in the range $C>0.4$, good agreement is obtained for the dependence of the Hall mobility on the metal concentration in the range $0.4<C<0.9$, as is evident from Fig. 10. In the lower concentration range $C<0.4$ the EMT-z results in a minimum in the μ-vs-C curve at $C^*_{\mathrm{EMT}}=\frac{1}{3}$. The EMT-$z$ fails in the low C range (<0.4). This is also evident from the behavior of μ expected from Eq. (3.18). As numerical simulations for R and μ are not available, we have compromised by using a hybridized theory (HT), expressing μ in terms of Eq. (3.15) with $\bar{f}$ derived from numerical simulations. The resulting curve, labeled as the HT in Fig. 11 results in a minimum at $C^*\simeq0.17$. It appears that for an inhomogeneous material characterized by a low value of x and a high value of $y\sim1$, the Hall mobility

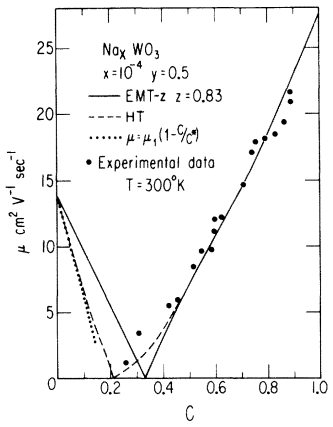

FIG. 11. Analysis of the Hall mobility data (Refs. 9 and 10) for Na_xWO_3 at 300 °K. Solid lines represents the results of the EMT-Z $x=10^4$, $y=0.5$ and $z=0.83$. Dashed line corresponds to the HT. Dotted line for $C \leq 0.1$ corresponds to Eq. (3.19).

will exhibit a minimum in the vicinity of the continuum percolation threshold.

IV. CONCLUDING REMARKS

We believe we have built up strong evidence for the nonrandom clustering model in alkali-tungsten bronzes. In this material, the metal-nonmetal transition proceeds via the inhomogeneous transport regime, where percolation effects result in a continuous change of the conductivity. The interpretation of the onset of the metal-nonmetal transition in terms of a threshold for continuous percolation is drastically different from the Mott transition in a microscopically homogeneous system, as in the present case the conduction electrons are always confined to locally metallic regions. There are common unifying features of the variation of the electronic structure and the transport properties in all microscopically inhomogeneous materials, such as the one component systems, expanded liquid Hg in the density range 9.2–8.0 g cm^{-3}, [26b] and liquid Te over the temperature range 1100–690 °K, [26a,41] and the two-component systems metal-ammonia solutions (MAS), in the metal concentration range 2.3–9 mole%, [25] and alkali-tungsten bronzes over the entire metal concentration range. In both MAS and in M_xWO_3 the correlation length b is independent of the metal concentration, the primary variable of state. In the former case there are bimodal concentration fluctuations, while in the latter microscopic metallic clusters are stabilized by a negative surface energy. It should, however, be noted that in liquid MAS b provides an average measure of the effects of dynamic local clustering, and the correlation length for concentration fluctuations will be temperature dependent, while in solid M_xWO_3 the cluster structure and therefore b are independent of temperature. It is quite remarkable that from a careful analysis of the conductivity data in M_xWO_3 we were able to obtain structural information concerning the M-M correlation length in this system. The value of $b \simeq 45$ Å for solid M_xWO_3 is considerably larger than for one and two component liquid systems studied by us, i.e., $b \simeq 15$ Å for expanded fluid Hg in the density range 9.2–8.0 g cm^{-3}, [26b] $b=4$ Å for Te in the temperature range 1100–690 °K, [41] and $b \simeq 15$ Å for Li-NH_3 solutions at 223 °K. [25b] The correlation length extracted from the transport data in M_xWO_3 should be subjected to a direct experimental test. Structural studies, such as small-angle x-ray and neutron scattering and electron microscopy, should be initiated to provide direct evidence for the existence of microscopic inhomogeneities in alkali-tungsten bronzes. Some electron microscopic studies already exist for $K_{0.2}WO_3$ in the hexagonal phase. [42] These show evidence for nearest-neighbor clustering of low occupancy channels of K sites of order 100 Å long or longer. There is also evidence for short-range ordering of these clusters with an average distance between them of 50 Å. Our isotropic approximation to the site correlation function represents a simplification of the observed structure.

ACKNOWLEDGMENTS

This research has been supported in part by the U. S. A. -Israel Binational Science foundation at the Tel-Aviv University and the ARO(D). We have also benefited from support of the Materials Research Laboratory of the National Science Foundation at The University of Chicago. We are indebted to Professor A. R. Mackintosh for helpful discussions and to Dr. S. Iijima and Dr. J. Cowley for permission to quote their unpublished results.

[1] F. Wohler, Ann. Chim. Phys. 29, 43 (1823).
[2] W. F. de Jong, Z. Kristallogr. 81, 314 (1932).
[3] M. E. Straumanis, J. Am. Chem. Soc. 71, 679 (1949); 71, 683 (1949).
[4] E. O. Brimm, J. C. Brantley, J. H. Lorentz, and M. H. Jellinek, J. Am. Chem. Soc. 73, 5427 (1951).
[5] J. F. Smith and G. C. Danielson, J. Chem. Phys. 22, 266 (1954).
[6] H. R. Shanks, P. H. Sidles, and G. C. Danielson, Adv. Chem. Ser. 39, 237 (1963).
[7] (a) M. J. Sienko, J. Am. Chem. Soc. 81, 5556 (1959); (b) Adv. Chem. Ser. 39, 294 (1963).
[8] L. D. Ellerbeck, H. R. Shanks, P. H. Sidles, and G. C. Danielson, J. Chem. Phys. 35, 298 (1961).
[9] L. D. Muhlstein and G. C. Danielson, Phys. Rev. 158, 825 (1967).

[10]P. A. Lightsey, Phys. Rev. B 8, 3586 (1973).
[11]W. R. Gardner and G. C. Danielson, Phys. Rev. 93, 46 (1954).
[12]B. W. Brown and F. Banks, J. Am. Chem. Soc. 76, 963 (1954).
[13](a) F. Kupka and M. J. Sienko, J. Chem. Phys. 18, 1296 (1950); (b) L. E. Comroy and M. J. Sienko, J. Am. Chem. Soc. 74, 3250 (1952).
[14]J. D. Greiner, H. R. Shanks, and D. C. Wallace, J. Chem. Phys. 36, 772 (1962).
[15]R. W. West, M. Grifeil, and J. F. Smith, J. Chem. Phys. 28, 295 (1958).
[16]R. Fuchs, J. Chem. Phys. 38, 1991 (1963).
[17]W. H. Jones, E. A. Garbaty, and R. G. Bernes, J. Chem. Phys. 36, 494 (1962).
[18]A. T. Fromhold, Jr. and A. Narath, Phys. Rev. 136, A481 (1964).
[19]A. T. Fromhold, Jr., and A. Narath, Phys. Rev. 152, 585 (1966).
[20]A. R. Mackintosh (private communication).
[21]D. E. Barmaal, R. G. Barnes, B. R. McCart, L. W. Mohn, and D. R. Torgeson, Phys. Rev. 157, 510 (1967).
[22]L. F. Mattheiss, Phys. Rev. B 6, 4718 (1972).
[23](a) A. R. Mackintosh (private communication) has pointed out that the calculations of Ref. 22 for $KMoO_3$ are not internally self-consistent, as the potential is constructed from atomic charge densities locating one electron in each K 4*s* orbital, while the final result is that complete electron transfer from K sites to the Mo 5*d* band occurs. (b) A. R. Mackintosh (private communication) prefers a picture where partial electron transfer from the alkali atom to the 5*d* band occurs.
[24]S. M. Marcus and T. A. Bither, Phys. Rev. Lett. 23, 1381 (1969).
[25](a) J. Jortner and Morrel H. Cohen, J. Chem. Phys. 58, 5170 (1973); and (b) (unpublished).
[26](a) Morrel H. Cohen and J. Jortner, Phys. Rev. Lett. 30, 699 (1973); (b) Phys. Rev. A 10, 978 (1974); and (c) in *Proceedings of the Fifth International Conference on Amorphous and Liquid Semiconductors* (Taylor and Francis, Garmisch, 1974), p. 167; and (d) J. Phys. (Paris) 35, C4-345 (1974).
[27]N. F. Mott and E. A. Davis, *Electronic Processes in Noncrystalline Materials* (Clarendon, Oxford, 1971).
[28]A. R. Mackintosh, J. Chem. Phys. 38, 199*i* (1963).
[29]S. Kirkpatrick, Phys. Rev. Lett. 27, 1722 (1971).
[30]S. Kirkpatrick, Rev. Mod. Phys. 45, 574 (1973).
[31]S. Kirkpatrick, in *Proceedings of the Second International Conference on Liquid Metals, Tokyo*, 1972 (Taylor and Francis, London, 1972).
[32]D. J. Thouless and B. J. Last, Phys. Rev. Lett. 27, 1719 (1972).
[33]V. K. S. Shante and S. Kirkpatrick, Adv. Phys. 20, 325 (1971).
[34](a) R. Zallen and H. Scher, Phys. Rev. B 4, 4471 (1971); (b) A. S. Skall, B. I. Shklovskii, and A. L. Efros, Zh. Eksp. Teor. Fiz. Pis'ma Red. 17, 522 (1973) [JETP Lett. 17, 377 (1973)].
[35]I. Webman, J. Jortner, and Morrel H. Cohen, Phys. Rev. 8, 2885 (1975).
[36]H. Weyl, Math. Ann. 71, 441 (1911).
[37](a) D. A. G. Bruggeman, Ann. Phys. (Leipzig) 24, 636 (1935); (b) V. I. Odelevskii, J. Tech. Phys. (USSR) 21, 678 (1961); (c) R. Landauer, J. Appl. Phys. 27, 838 (1956).
[38]H. L. Crowder and M. J. Sienko, J. Chem. Phys. 38, 1576 (1963).
[39]See, for example, J. M. Ziman, *Electrons and Phonons* (Oxford U. P., New York, 1961).
[40]Morrel H. Cohen and J. Jortner, Phys. Rev. Lett. 30, 696 (1973).
[41]Morrel H. Cohen and J. Jortner (unpublished).
[42]S. Iijima (private communication). We are grateful to Dr. R. Silberglitt for calling this work to our attention.